



IPOMOEA PES-CAPRAE FLOWER EXTRACT-BASED GREEN SYNTHESIS OF PURE ZINC OXIDE NANOPARTICLES: ANALYSIS OF THE STRUCTURAL, OPTICAL, MORPHOLOGICAL, AND BIOMEDICAL FEATURES

^{1,2}Mary Harli Mol, ^{2,3}Dr. S. Ajin Sundar,

¹Research Scholar (Reg. no: 19213232132007), PG & Research Centre, Department of Physics, St. Jude's College, Thoothoor, Tamil Nadu – 629176, India.

²Manonmanium Sundaranar University, Tirunelveli, Tamil Nadu – 627012, India.

³Assistant professor, Department of Physics, St. Jude's College, Thoothoor, Tamil Nadu – 629176, India.

Abstract:

The current effort aims to develop two different concentrations of Ipomoea pes-caprae flower extract as a biological source for the production of ZnO nanoparticles (ZnO NPs) in a safe and ecologically friendly manner. A variety of techniques were carried out to characterize the prepared ZnO nanoparticles, such as the MTT assay, X-ray diffraction(XRD), Fourier transform infrared spectroscopy(FTIR), UV-diffuse reflectance spectroscopy(UV-DRS), and Energy dispersive X-ray analysis (EDX). The XRD analysis revealed that the prepared ZnO nanoparticles exhibit a hexagonal Wurzite shape. The crystallite's size got increases from 30.3nm to 40.5 nm as the concentration ratio increased. At 467.95 cm⁻¹ and 467.81 cm⁻¹, FTIR spectroscopy confirms the formation of ZnO. UV-diffuse reflectance spectroscopy indicates the band gap lower from 3.05 eV and 2.92 eV as the concentration rises. FE-SEM studies were utilised to evaluate the obtained ZnO nanoparticles' structure, reveal nano spherical-shaped structures. According to the EDAX analysis, the produced sample solely included zinc and oxygen. The synthesised ZnO nanoparticle showed significant antifungal effectiveness against Candida tropicalis and Aspergillus niger, as well as high antibacterial performance over Staph albus (Gram-positive) and Vibrio cholera (Gram-negative). The MTT experiment proved that cell viability decreased as ZnO concentration increase.

1) Introduction

Nanotechnology has emerged as the newest area of study since it has applications across many branches of science, such as electronics, optics, biology, and material science [1]. It is defined as the creation, analysis, and research of materials in the nanoscale range (1- 100 nm) [2]. The high surface-to-volume ratio of nanoparticles is one of their distinctive characteristics, which adds an additional attraction to them. [3]. When compared to bigger particles of bulk materials, nanoparticles exhibit entirely new or better qualities. These innovative features result from variations in the size, dispersion, and shape of the particles. [4]. Metal oxide (MO) NPs are regarded as the foremost potential of all the types of NPs now available due to their distinct physical, chemical, and biological features, including solubility, chemical stability, and adhesiveness. [5]. Metal oxide nanoparticles (NPs) are the most commonly employed

nanomaterials in biomedicine to treat a variety of diseases [6, 7]. Metal and metal oxide nanoparticles have garnered significant interest across various fields owing to their manifold advantageous properties, encompassing catalytic, optical, electrical, and magnetic functionalities [8]. Among the well-established inorganic materials with antibacterial properties, metallic nanoparticles (NPs) and metal oxide NPs like silver, gold, copper, titanium oxide, and zinc oxide (ZnO) stand out as notable examples. [9].

One of the metal oxide nanoparticle that has recently piqued scientific interest is zinc oxide [10]. ZnO is a multifunctional II-IV composite semiconductor that possesses exceptional qualities such as low cost, reliability, low toxicity, thermal stability, and material availability. The US-FDA department has designated it as a substance that is "Generally Recognized as Safe" (GRAS) [11]. ZnO's unique characteristics, such as its hardness, stiffness, and piezoelectric constant, demonstrate its significance as a material in the ceramics sector [12]. ZnO nanoparticles are a highly advanced substance that have been employed for a variety of useful purposes, such as antimicrobial activities, cosmetics, and wastewater treatment catalysis [13]. The synthesis of the materials is a prerequisite for any novel investigation of nanoparticles. Currently, it is difficult to develop comprehensive studies for the preparation of ZnO nano materials [14] [15]. In order to prepare ZnO nanoparticles, many procedures have been invented, including sol-gel [16], wet chemical [17], co-precipitation [18], thermal breakdown [19], solid-state reaction [20], hydrothermal [21], and solvothermal approaches [22]. Limitations associated with these synthesis techniques include the use of toxic chemicals, pricey steps, and difficult reaction environments [23]. Furthermore, the nanoparticle production procedure entails the use of toxic substances as both capping and reduction agents, resulting in negative impacts on the environment, organisms, and plant life [24, 25]. The rapidly expanding recognition of environmentally friendly practises in the present culture has made it possible to create nanoparticles using a green approach [26]. Green synthesis is a very efficient method for producing nanomaterials on an extensive basis and can remove significant quantities of potentially dangerous chemicals [27, 28]. Natural plant extracts are rich in advantageous phytochemicals that serve as potent agents for reducing, stabilizing, and capping nanoparticles during their production. [29].

Plant-mediated nanoparticle manufacturing can take place both inside and outside of plant cells. The extracellular method involves using a plant extract made by heating and

crushing the plant in a solvent or aqueous solution, whereas the intracellular approach entails cultivating in metal-enriched organic environments [30]. Based on earlier reports in the literature, ZnO NPs have been biosynthesized from various types of natural-based renewable sources, for instance, plant extract, bacteria and yeast, are used as alternatives to replace the toxic chemicals [31]. Eco-friendly synthesis of ZnO NP by micro-organisms such as *Lactobacillus*, *Bacillus subtilis* and *E. coli* [32] and several plant extracts such as *Cayratia pedata* leaf extract [33], *Loures Nobilis* leaf extract [34], *Hibiscus sabdariffa* leaf extract [35], *Acalypha indica* leaf extract [36], *Tecoma castanifolia* leaf extract [37], *Ipomoea pes-caprae* leaf extract [38], *Olea europaea* leaf extract [39].

2) Materials and methods

2.1) Materials

Analytical-grade zinc nitrate hexahydrate ($Zn(NO_3)_2 \cdot 6H_2O$) was furnished by Sig- ma-

Aldrich, and triple-distilled deionized water was used to prepare all aqueous solutions. The flowers of *Ipomoea pes-caprae* were employed as both a reducing and stabilising agent in the environmentally friendly bio-reduction synthesis of ZnO nanoparticles (NPs).

2.2) Preparation of *Ipomoea pes-caprae* flower extract

Ipomoea pes-caprae's fresh flowers were extensively cleansed in sterile, double-distilled water to get rid of the dirt. After allowing the fresh flowers to undergo a three-day period of shade drying, 10 grams of the resulting dried flowers were dissolved in 100 milliliters of distilled water using a magnetic stirrer-heater. Subsequently, the mixture was heated within the temperature range of 50 to 60 degrees Celsius for a duration of 60 minutes. Whatman No. 1 filter paper was used for filtration in order to separate the extract. [44].

2.3) Green synthesis of ZnO nanoparticles

In the process of producing ZnO nanoparticles, a gradual and drop-wise addition of 10 mL of *Ipomoea pes-caprae* flower extract was made into a 60 mL solution containing 0.1 M $\text{Zn}(\text{NO}_3)_2 \cdot 6\text{H}_2\text{O}$. The blend underwent uninterrupted stirring for a duration of 3 hours. The resultant solution was then centrifuged for 20 minutes at a speed of 4000 rpm. To remove any extra $\text{Zn}(\text{NO}_3)_2 \cdot 6\text{H}_2\text{O}$ and any lingering organic compounds, the residue was then washed with deionized water. Additionally, it underwent a 3-hour drying phase in an oven set at 70°C, and subsequently, it was subjected to a 3-hour calcination process in a furnace at 450°C in order to produce ZnO nanoparticles. The resulting particles were gathered and given the name ZnO-A. In the instance of ZnO-B samples, an identical procedure was carried out using 15 mL of *Ipomoea pes-caprae* flower extract.

2.4) Characterization

The powder X-ray diffraction was performed to analyse the structure of the prepared samples by using a Powder X-ray Diffractometer (PANalytical X'Pert PRO) with $\text{Cu-K}\alpha$ radiation source (1.5406 Å). FTIR spectral analysis (Make: Perkin Elmer), UV-Diffuse reflectance spectroscopy (Varian Cary 5000) and Raman spectroscopy [Raman Spectroscopy Agilentron, USA] were used to analyse the optical properties of the prepared ZnO-A and ZnO-B. The morphological characteristics and elemental properties were analysed using Field emission scanning electron microscopy (FE-SEM) (Bruker).

3) Results and Discussion

3.1) Powder X-Ray Diffraction (XRD)

The crystalline phase and structural properties of prepared ZnO nanoparticles were examined by using Powder XRD analysis. The XRD image of the generated ZnO samples at two different concentrations is shown in Figure 1. The diffractogram shows the intensity of the diffracted rays as a function of diffraction angles. The XRD diffraction peaks existed at 2θ angles of 31.9°, 34.6°, 36.4°, 47.8°, 56.7°, 62.9°, 66.5°, 68°, 69.2°, 72.7°, 76.9° corresponding to lattice plane (100) (002) (101) (102) (110) (103) (200) (112) (201) (004) (202) depicts the hexagonal wurzite structure of ZnO per JCPDS (card no.: 89-1397) standards. The high purity as well as the fine crystalline nature of the prepared ZnO-A and ZnO-B samples are confirmed by the sharp, vivid peaks of ZnO. The XRD patterns of ZnO-A nanoparticles typically show broad peaks. According to the literature [45, 46], the broad peak is an indication of small and fine NPs. The XRD patterns of ZnO-B nanoparticles typically higher crystallinity and sharper

XRD peaks. The extract concentration influences the size and the crystal structure of ZnO nanoparticles, which in turn affects the intensity of the XRD peaks. The peak broadening can be reduced, indicating an increase in the degree of crystallinity of the material. The ZnO nanoparticles' crystallite size (D) was estimated using Debye Scherrer's formula from the reflection peak with the highest intensity, which corresponds to the (101) planes.

$$D = \frac{0.9\lambda}{Q\cos\theta}$$

Where,

- 'λ' is the X-ray wavelength used for diffraction,
- 'β' is the Full Width Half Maximum, and
- 'θ' is the Bragg's angle.

The computed crystallite size of the prepared sample ZnO-A and ZnO-B are 30.3nm and 40.5 nm. The nanoparticles' crystallite size increases along with the increasing concentration of Ipomoea pes-caprae flower extract. According to past studies, the ratio of concentrations has a substantial impact on the sizes and morphology of the prepared ZnO (A, B) nanoparticles [47].

The produced ZnO-A and ZnO-B nanoparticle particles are recognised as having a wurzite hexagonal densely packed structure based on the XRD pattern. The following equation was used to calculate the lattice constants a and c by applying the interplanar distances d and hkl values of the XRD pattern:

$$\frac{1}{d^2} = \frac{4}{3} \left\{ h^2 + hk + \frac{l^2}{a^2} \right\} \frac{l^2}{c^2}$$

The estimated lattice parameters, which are listed in table 1, closely resemble those provided in the typical JCPDS data.

SAMPLE	CRYSTALLITE SIZE (D)	LATTICE CONSTANT (A)	LATTICE CONSTANT (C)	DISLOCATION DENSITY (Δ)
ZNO-A	40.5 nm	3.23179	5.18112	0.000694694
ZNO-B	30.3 nm	3.23120	5.17551	0.000913587

Table 1. ZnO (A, B) nanoparticle structural variables.

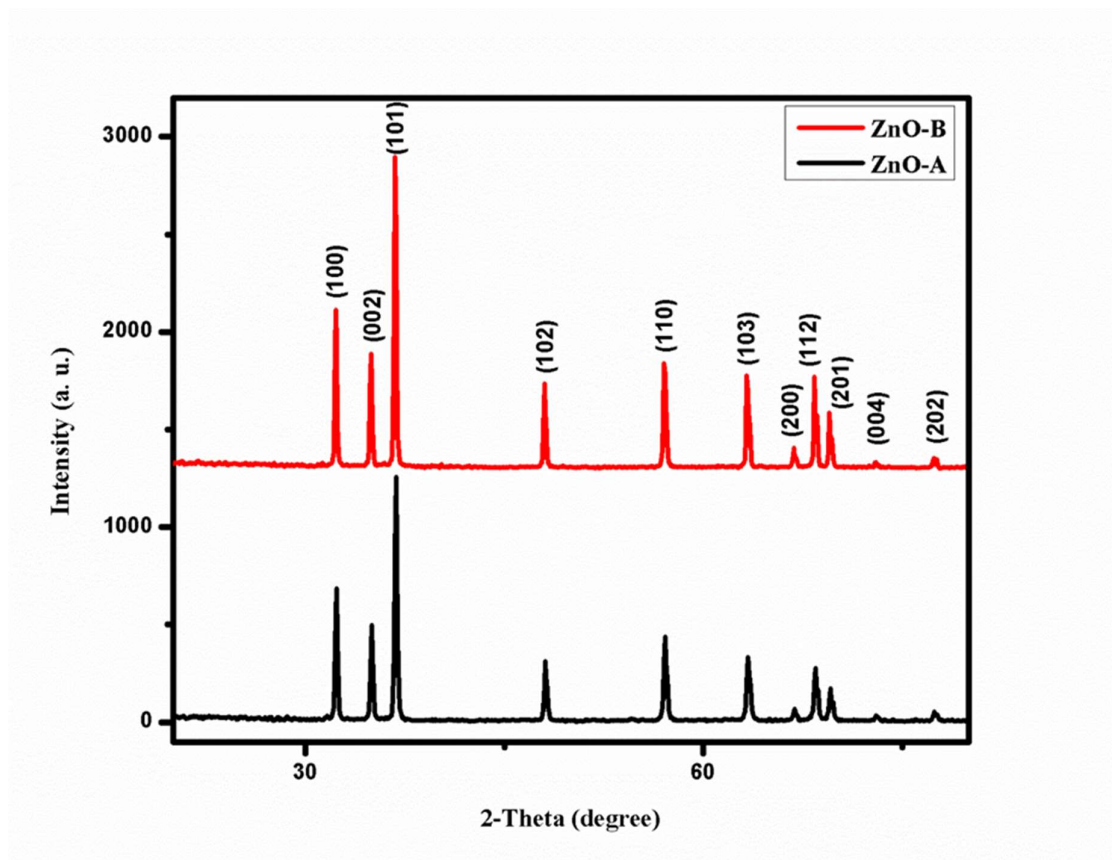


Fig. 1 XRD spectra of the green synthesised ZnO nanoparticles at ZnO-A and ZnO-B.

The number of dislocation in the lattice of the ZnO crystal were measured using the dislocation density. The measured dislocation density of the prepared ZnO-A and ZnO-B samples are also given in Table 1. The increase in dislocation density was observed in ZnO nanoparticles.

3.2) FT-IR Analysis

Through the use of FTIR spectroscopy, the functional group's existence in the synthesised ZnO-A and ZnO-B nanoparticles was discovered. The FTIR spectra of the produced

ZnO (A, B) nanoparticles, with wavenumbers ranging from 400 cm^{-1} to 4000 cm^{-1} , are shown in Figure 2. Moreover, it indicates that the collaborative interaction of phenolic compounds, alkynes, terpenoids, and flavonoids leads to the formation of ZnO nanoparticles.

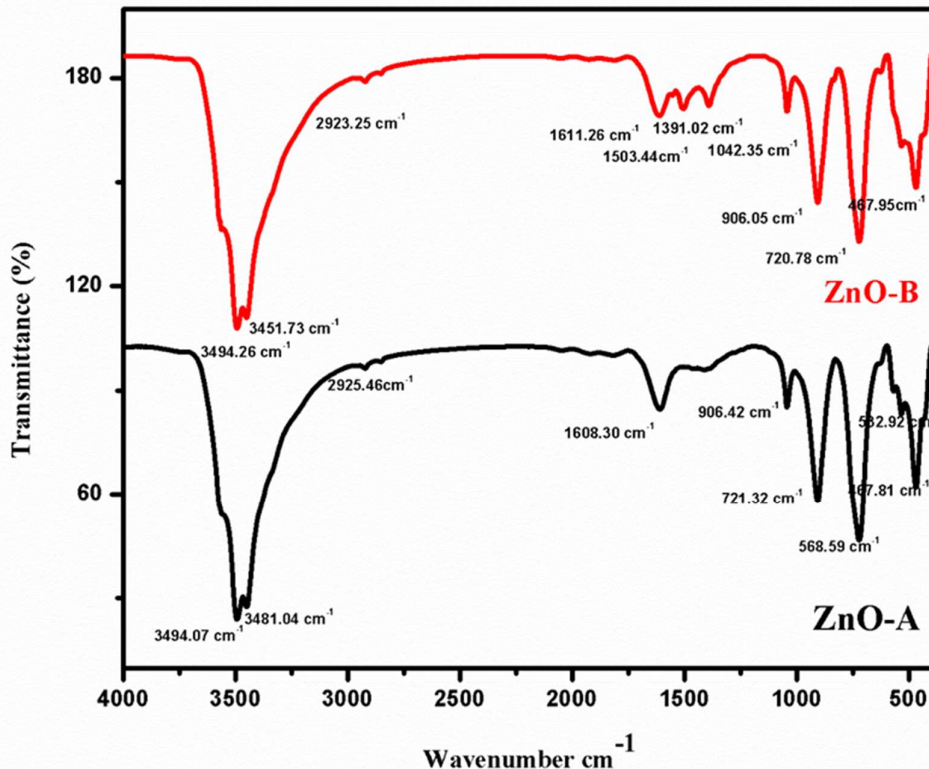


Fig. 2 FTIR spectra of the green synthesised ZnO nanoparticles at ZnO-A and ZnO-B.

The broad peaks observed at 3451.73 cm⁻¹, 3494.26 cm⁻¹, 3481.04 cm⁻¹, and 3494.07 cm⁻¹ in the spectra of both ZnO-A and ZnO-B nanoparticles are a result of the presence of water molecules on their surfaces. These peaks correspond to O-H stretching, which is consistent with the characteristics of phenolic compounds. The tiny peaks detected at 2923.25 cm⁻¹ and 2925.46 cm⁻¹ arise from the C-H stretching vibrations within the alkane group. The small, subtle peaks at 1611.26 cm⁻¹, 1608.30 cm⁻¹, and 1506 cm⁻¹ can be attributed to the stretching vibrations of the C=C bonds. The IR areas of 467.95 cm⁻¹, 467.81 cm⁻¹, and 582.92 cm⁻¹ displayed the Zn-O stretching mode. These stretching mode peaks are evidence of the effective production of ZnO nanoparticles. The existence of bands at 3451.73 cm⁻¹, 3494.26 cm⁻¹, 3481.04 cm⁻¹, 3494.07 cm⁻¹, 1627 cm⁻¹, and 1506 cm⁻¹ indicates that proteins, phenols, terpenoids, and flavonoids, which include functional groups like alcohols, are participating in bioreduction reactions.

3.3) UV-Diffuse Reflectance Spectroscopy

The optical properties of the generated ZnO-A and ZnO-B nanoparticles were investigated using the UV-DRS spectrum. Figure 3, illustrates the UV diffuse reflectance spectrums of prepared ZnO-A and ZnO-B nanoparticles. In the current context, the spectra of the green synthesised nanoparticles were examined within the wavelength range of 200 to 800 nm.

UV-Visible Diffuse Reflectance Spectroscopy (UV-Vis DRS) offers direct evidence of the

light-absorbing capacity of ZnO-A and ZnO-B nanoparticles synthesized using green methods. The ZnO-A sample fully reflects all visible light (100%), whereas the ZnO-B sample reflects light to a slightly lower extent (85%).

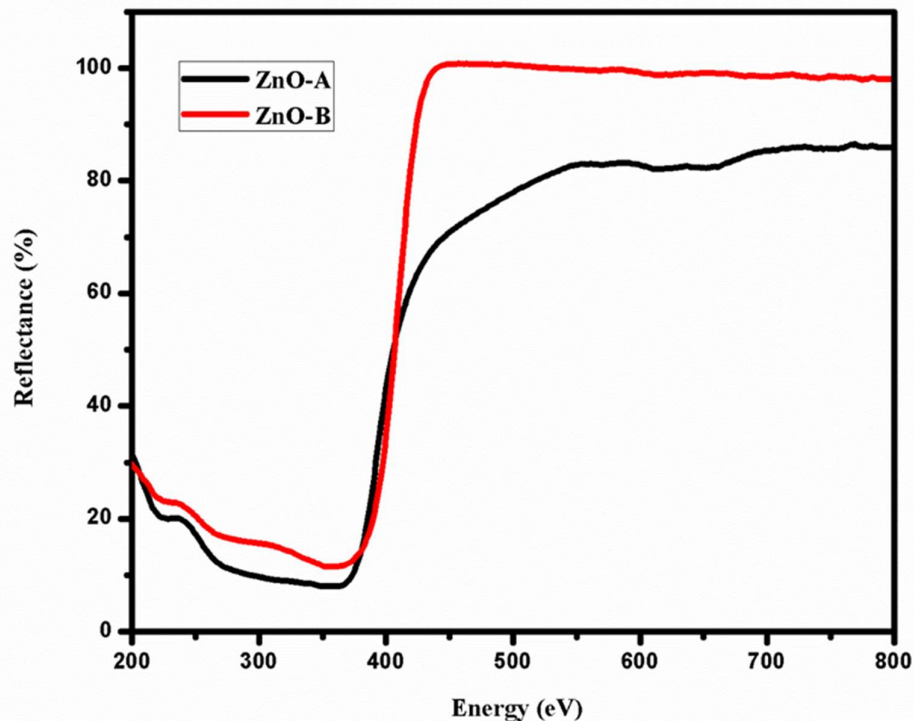


Fig. 3 UV-DRS spectra of the green synthesised ZnO nanoparticles at ZnO-A and ZnO-B.

The produced samples, ZnO-A and ZnO-B, show a substantial increase in the UV diffuse reflectance spectra at 390 nm and 385 nm, respectively. The produced samples' absorption spectra were determined from the reflection data using the following Kubelka-Munk (K-M) function:

$$F(R) = \frac{(1 - R)^2}{2R}$$

Where R stands for reflectance.

The bandgap values were calculated from the plot of the modified Kubelka-Munk function $(F(R) E)^{1/2}$ vs. the energy of the adsorbed light (E) using linear fits close to the absorption edge shown in figure 4 [48–50]. ZnO-A and ZnO-B's computed band gaps were 3.05 eV and 2.92 eV, respectively. This shows that the resulting bandgap of the synthesised ZnO nanoparticles is influenced by the extract's volume. [47]. These numbers are comparable to those that were already reported for ZnO NPs [51]. In comparison to the bulk ZnO (3.37 eV), the estimated band gap values of the produced ZnO-A and ZnO-B samples are smaller. This is

true because the blue shift in excitonic absorption favors a ZnO-A and ZnO-B samples are smaller little quantum confinement effect.

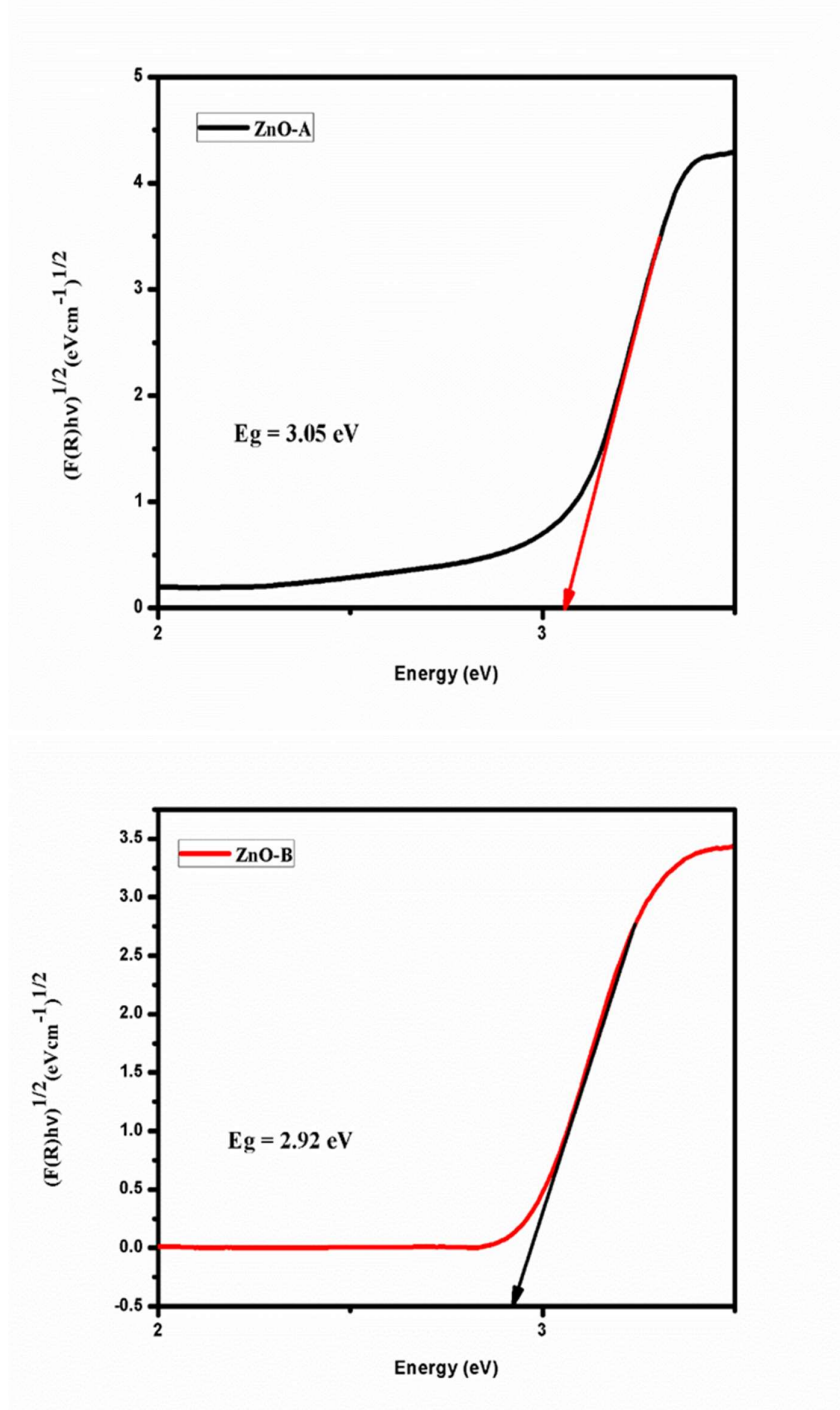


Fig.4 Kubelka-Munk graph for determining the band gap of the green synthesised ZnO nanoparticles at ZnO-A and ZnO-B.

As per the provided findings, the band gap values of the synthesised ZnO-A and ZnO-B nanoparticles decreased with an increase in the concentration of the Ipomoea pes-caprae flower extract.

3.4) FE-SEM with EDAX

Field emission scanning electron microscopy (FE-SEM) was used to analyse the morphology of the produced ZnO-A and ZnO-B nanoparticles. Figure 5 shows the FE-SEM image of the prepared ZnO-A and ZnO-B samples. FESEM images were acquired with a magnification of 200 nanometers to assess the size and structural characteristics of the nanoparticles. The ZnO-A sample's FE-SEM picture reveals spherical forms with aggregation. The ZnO-B sample, in contrast, displays a spherical shape with less aggregation. When Ipomoea pes-caprae flower extract concentration is increased, the aggregation appears to decrease, maintaining the particles' spherical shape. The 15 mL Ipomoea pes-caprae flower extract has a sufficient amount of phytochemicals to successfully decrease and cap the ZnO nanoparticles. Based on the literature review [47], lower amounts of plant extract may produce larger, more agglomerated ZnO nanoparticles, while higher concentrations may produce smaller, more uniform ZnO nanoparticles.

Energy dispersive spectroscopy of ZnO-A prepared by green synthesis method shown in the figure 6. Our available data offers evidence of the presence of Zn and O, as indicated by their respective weight percentages. The EDAX measurement only exposes the peaks of zinc and oxygen, proving that the manufactured ZnO nanoparticles are free of impurities.

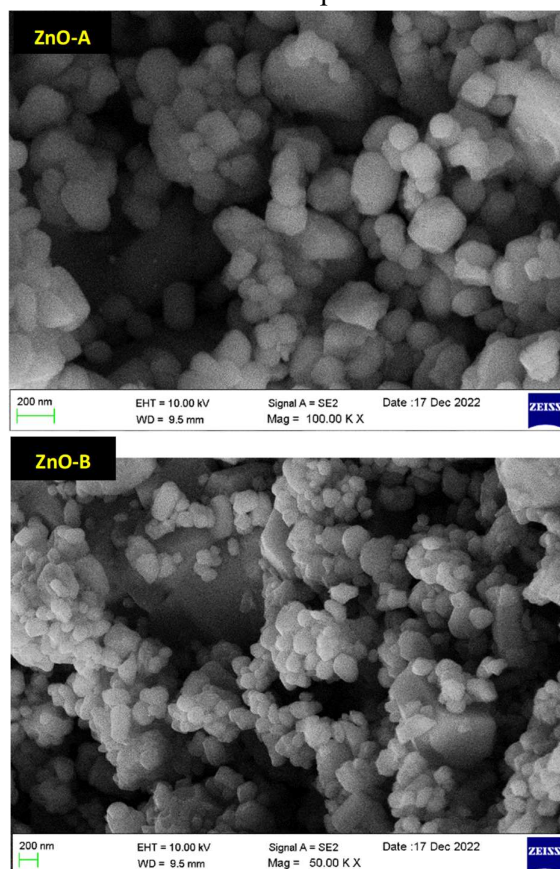


Fig. 5 FE-SEM Micrograph of the green synthesised ZnO nanoparticles at ZnO-A and ZnO-B.

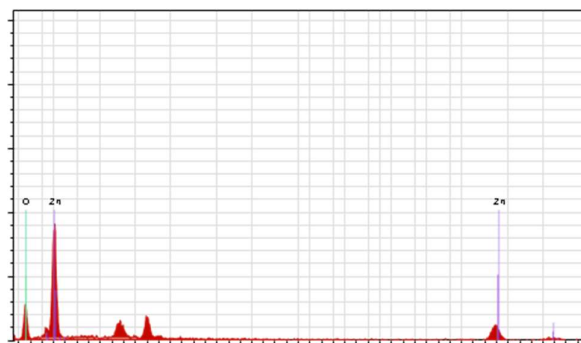


Fig. 6 EDAX image of the green synthesised ZnO nanoparticles at ZnO-A.

3.5) DLS Analysis

Dynamic light scattering, often known as DLS, is a method for determining the size and size distribution of nanoparticles in a fluid. Additionally, DLS can reveal details regarding the stability, aggregation, and morphology of nanoparticles. In this investigation, the DLS method was used to determine the size distribution and average particle size of biosynthesized ZnO NPs. The DLS spectra of the greenly synthesised nanoparticles ZnO-A and ZnO-B are shown in Figure 7. According to DLS spectra, the average particle sizes of ZnO-A and ZnO-B nanoparticles produced by green synthesis were 188 nm and 151.9 nm, respectively, with polydispersive values of 0.248 and 0.231. The agglomeration or expansion of nanoparticles as well as the emergence of new phases or crystalline structures are both responsible for the alterations in the DLS spectra.

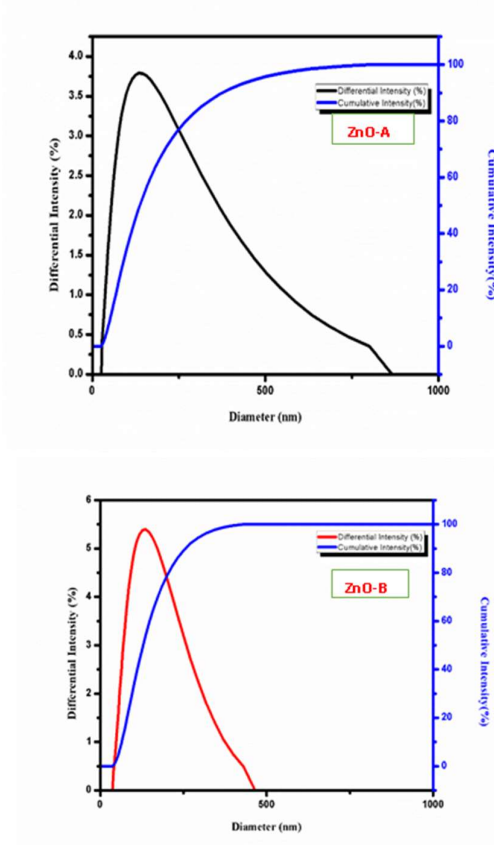


Fig. 7. DLS Spectra of the green synthesised ZnO nanoparticles at ZnO-A and ZnO-B.

3.6) Biomedical Applications

It is well known that all biological tissues contain a sizable amount of zinc, a crucial micro mineral. ZnO NPs, which are substantially less expensive and hazardous than other metal oxide NPs, have excellent medicinal applications in the treatment of diabetes, cancer, drug delivery, and other bacterial and inflammatory conditions, as well as wound healing and bio imaging. The biomedical applications of the green synthesised ZnO NPS were tested on the best sample (ZnO-A) out of the two prepared samples.

3.6.1) Anti-bacterial and Anti-fungal Characterization

The antibacterial and antifungal efficacy of the produced ZnO-A sample was evaluated using the Kirby-Bauer disc diffusion method, also known as the Kirby-Bauer methodology.

Kirby-Bauer method:

According to the manufacturer's instructions, the medium is prepared and sterilized. Prior to inoculation, the plates were allowed to air-dry with their lids slightly open to ensure that no moisture droplets were present on the surface of the agar. The specific bacteria are touched with a wire loop from the agar medium, and the growth is transferred to a test tube containing 1.5 ml of sterile, appropriate broth. To create a moderately turbid bacterial suspension, the tubes are incubated for two hours between 35°C and 37°C. On Muller-Hinton agar plates, bacteria were swabbed after being cultured to 0.5 McFarland standards. At room temperature, the agar medium was then allowed to cool and solidify in a petri dish with a depth of 3 mm. Sterilised forceps were employed to position the filter paper discs infused with nanoparticles onto the inoculated petri dishes. Each disc was filled with 20 L of that specific NP solution and allowed to air dry. Plates are incubated under aerobic conditions at 35–37 °C for 16–18 hours in the presence of meticulous microbes. The areas of inhibition around the disc were noted, and the corresponding diameters were calculated. The antibacterial and antifungal abilities of the ZnO-A sample were examined three times for the best results.

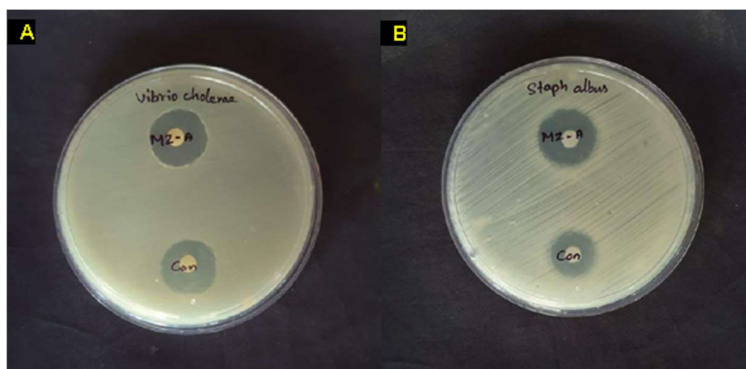


Fig. 8 Antibacterial study of ZnO-A NPs illustrating an area of inhibition of the growth of (A) *Vibrio cholerae* and (B) *Staph albus*.

Figure 8, depicts the green synthesised ZnO-A nanoparticles' growth and inhibition against pathogenic bacteria using Kirby-Bauer disk diffusion method. The Gram-positive *Staph albus*

and the Gram-negative *Vibrio cholera* were used as targets for the ZnO-A nanoparticles' antibacterial activity. Drug Amikacin used as a positive control for the comparison of ZnO NPs. The zone of inhibition of ZnO-A NPs was observed for 20mm in *Vibrio Cholerae* and 21mm in *Staph albus*. On the other hand the positive control Amikacin showed the radius of the zone of inhibition of 19mm and 17mm against *Vibrio Cholerae* (Gram negative) and *Staph albus* (Gram positive).

The produced ZnO-A NPs showed antibacterial action towards both types of bacteria. However, it worked better on Gram-positive bacteria than it did on Gram-negative ones [55-57]. In contrast to gram-positive bacteria, gram-negative bacteria have an additional outer membrane made of Lipopoly saccharides (LP). LPS has been found to improve the outer membrane's barrier capabilities, increasing bacterial resistance in general and antibiotic resistance in particular [58]. Antibacterial activity of flower extracts might be due to the presence of chemical constitutions in the extracts [59]. Moreover, the synthesized ZnO-NPs of bioflavonoid rutin displayed moderate antibacterial activity [60].

BACTERIA	INHIBITION ZONE	CONTROL
VIBRIO CHOLERAEE	20mm	19mm
STAPH ALBUS	21mm	17mm

Table 2. ZnO-A NPs' antibacterial performance values against *Staph albus* and *Vibrio cholera*.



Fig. 9 Antifungal study of ZnO-A NPs illustrating an area of inhibition of the growth of (A) *Candida tropicalis*, (B) *Aspergillus niger*.

The green synthesized ZnO-A nanoparticles' antifungal potential using Kirby-Bauer disk diffusion method was shown in the Figure 9. The produced ZnO-A NPs' antifungal properties were tested using the fungi *Aspergillus niger* and *Candida tropicalis*. Drug Nystatin used as a positive control for the comparison of ZnO NPs. The anti-biotic inhibition was measured as 18mm for both *Aspergillus niger* and *Candida tropicalis* fungus, in the mean while the positive control Nystatin showed the radius of the zone of inhibition of 16mm respectively. On the basis of the results it was determined that the ZnO-A nanoparticle significantly inhibited the growth of the fungus *Candida tropicalis*, and *Aspergillus niger*.

FUNGUS	INHIBITION ZONE	CONTROL
CANDIDA TROPICALIS	18mm	16mm
ASPERGILLUS NIGER	18mm	16mm

Table 3. Antifungal measurements of ZnO-A NPs Candida tropicalis and Aspergillus niger.

ZnO NPs produced through the green synthesis method exhibit higher effectiveness compared to other preparation methods. This could be attributed to the release of oxygen species on the surface of ZnO, leading to lethal damage to microorganisms [61]. The prior research [62] demonstrated that the process of antifungal activity resembled the process of antibacterial activity, wherein the presence of greenly produced ZnO nanoparticles and reactive oxygen species (ROS) may be responsible for the rupture of fungal and bacterial cell membranes and the inhibition of cell development. According to the literature, it has been observed that ZnO is unstable in a solution, and its decomposition can lead to the production of H₂O₂. As ZnO decomposes, there is an increase in the concentration of Zn²⁺ ions. [63-65].

The cell is harmed by this process in a variety of ways, including DNA damage, protein denaturation, cellular respiration problems, cell membrane damage, and more.

3.6.2) MTT Assay study

The MTT test measures cell viability, proliferation, and cytotoxicity by measuring cellular metabolic activity. A yellow tetrazolium salt (3-(4, 5-dimethylthiazol-2-yl)-2, 5-diphenyltetrazolium bromide, or MTT) is transformed into purple formazan crystals in this colorimetric assay by metabolically active cells.

After being plated on 96-well plates with SKMEL (2500 cells per well), the cells were given 24 hours to acclimatise to the incubator's 37 °C and 5% CO₂ growth conditions. The test specimens were created in DMEM medium (100 mg/mL), and a 0.2 m Millipore syringe filter was used to sterilise the filter. Following another DMEM media dilution, the samples were added to the wells containing the growing cells at the desired concentrations of 6.25, 12.5, 25, 50, and 100 g/mL, respectively. Wells that hadn't been treated served as the benchmark.

Each experiment was run three times, and the average findings were used to eliminate inaccuracies. When the test samples were applied, the plates underwent another round of incubation for another 24 hours. The wells' media were aspirated after the incubation period and frequently thrown out. Every single well was filled with 100 L of a PBS solution that included 0.5 mg/mL MTT. Formazan crystals were then produced by leaving the plates in the reaction for two more hours. Each well received 100 L of 100% DMSO after the supernatant was removed. A microplate reader was used to determine the absorbance at 570 nm. The formula used to express cell viability is given below:

$$\text{Percentage of Viability} = \frac{\text{Average absorbance of treated}}{\text{Absorbance of control}} \times 100\%$$

SAMPLES	TRIPLICATE 1	TRIPLICATE 2	TRIPLICATE 3	AVERAGE
CONTROL	0.677	0.671	0.656	0.668
6.25	0.633	0.625	0.617	0.625
12.5	0.584	0.571	0.565	0.573
25	0.495	0.486	0.477	0.486
50	0.395	0.416	0.407	0.406
100	0.298	0.309	0.315	0.307

CONCENTRATION ($\mu\text{G/ML}$)	PERCENTAGE OF VIABILITY	IC 50
6.25	93.56	
12.5	85.82	
25	72.75	
50	60.77	
100	46	84.17

Table 4. MTT assay readings of various cell viability percentages versus various Concentrations

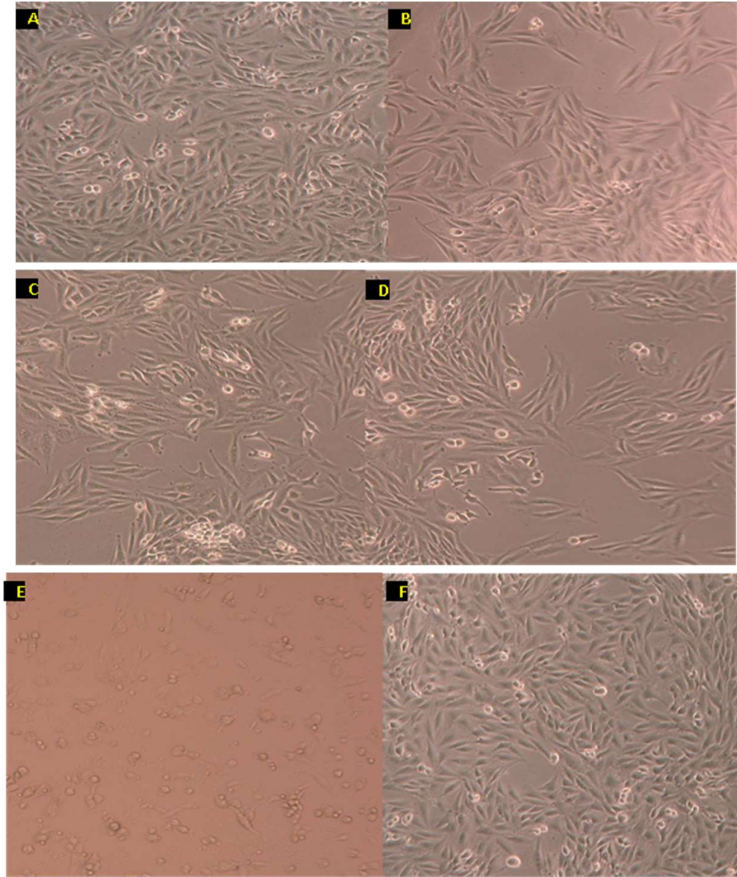


Fig. 10 Cell viability of SKMEL cancer cells with different concentrations of 6.25(A), 12.5(B), 25(C), 50(D), 100(D) $\mu\text{g}/\text{mL}$ and control (F) of the ZnO-A sample.

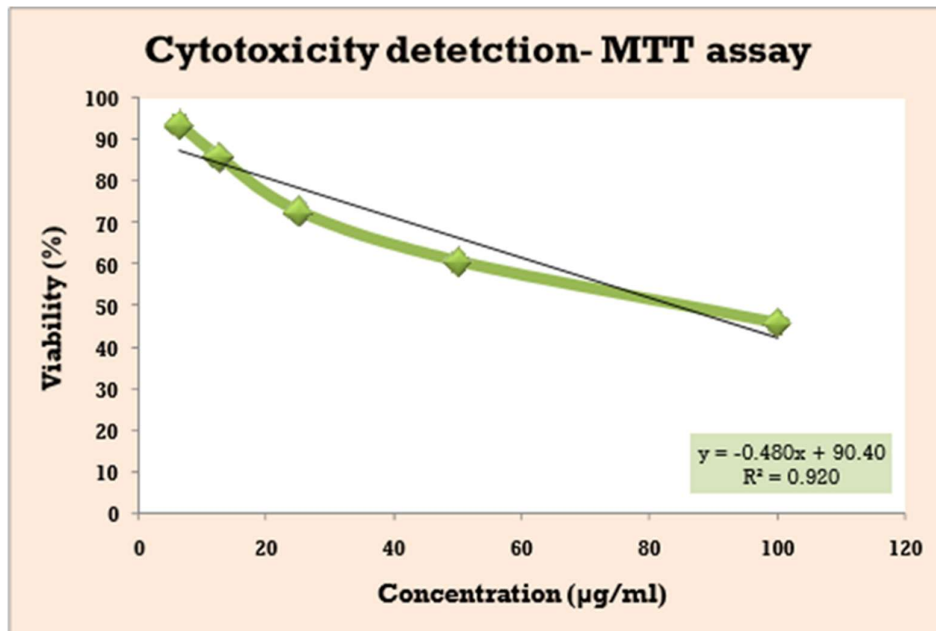


Fig. 11 MTT assay plot showing various percentages of cell viability versus various concentrations.

The half-maximum inhibitory concentration of the sample is known as the IC₅₀ value. The IC₅₀ value of ZnO nanoparticles was determined to be 84.17 g/ml. The viability of cells decreased with increasing ZnO nanoparticle concentration, is shown in figure 10 as well as in the above MTT assay result in figure 11. The alkaloids and flavonoids in the flower extract from *Ipomoea pes-caprae* may be responsible for the anticancer action [44]. According to our investigation, modest concentrations of ZnO NP had no impact on cell viability. Our research established the safety of ZnO NP at low concentrations in medical applications.

4) Conclusion

The eco-friendly green synthesis method was used to create the ZnO nanoparticle from two different concentration ratios of *Ipomoea pes-caprae* flower extract as a biological source. The resulting nanoparticles' structural, optical, and biological application features were studied. The produced ZnO (A, B) sample has a hexagonal wurzite structure, according to XRD measurements. Debye-Scherrer's equation was used to estimate the produced nanoparticles' crystallite sizes, which were found to be between 30.3nm and 40.5nm. At 467.95 cm⁻¹ and 467.81 cm⁻¹, FTIR spectroscopy shows the existence of ZnO. UV-diffuse reflectance spectroscopy shows that the band gap decreases with increasing concentration from 3.5 eV to 2.92 eV of *Ipomoea pes-caprae* flower extract. FESEM studies revealed the form of the produced ZnO nanoparticles. The DLS spectra analysis was used to determine the ZnO-A and ZnO-B nanoparticles' average particle sizes, as 188 nm and 151.9 nm with polydispersive values of 0.248 and 0.231. The prepared sample, which contains only zinc and oxygen, is verified by an EDAX analysis. The prepared ZnO nanoparticle demonstrated excellent antibacterial activity against *Staphylococcus albus* (Gram-positive) in comparison to *Vibrio cholera* (Gram negative), as well as significant antifungal activity against *Candida tropicalis* and *Aspergillus niger*. The MTT assay proves that cell viability decreased as ZnO concentration increased, and the ZnO NP is safe in medical applications at low doses.

Reference

- [1] Kato, H., "Tracking nanoparticles inside cells", *Nat. Nanotechnol.*, 6(3): 139-140 (2011).
- [2] Yadav, V., "Nanotechnology, big things from a tiny world: a review", *AEEEE* 3(6), 771-778 (2013).
- [3] B.D. Yao, Y.F. Chan, N. Wang, Formation of ZnO nanostructures by a simple way of thermal evaporation, *Appl. Phys. Lett.* 81 (2002) 757–759, <https://doi.org/10.1063/1.1495878>.
- [4] Ravindra P. Singh, Vineet K. Shukla, Raghvendra, S. Yadav, Prashant K. Sharma, Prashant K. Singh, Avinash C. Pandey (2011), Biological approach of zinc oxide nanoparticles formation and its characterization, *Advanced Materials Letters*, Vol. 2 No.4, pp.313-317.
- [5] Waseem, A.; Divya, K. Green synthesis characterization and anti-microbial activities of ZnO nanoparticles using *Euphorbia hirta* leaf extract. *J. King Saud Univ. Sci.* 2020, 32, 2358–2364.
- [6] D.Saravanakkumar, S.Sivaranjani, K.Kaviyarasu, A.Ayeshamariam, B.Ravikumar, S. Pandiarajan, C. Veeralakshmi, M. Jayachandran, M. Maaza, Synthesis and characterization of ZnO-CuO nanocomposites powder by modified perfume spray pyrolysis method and its antimicrobial investigation, *J. Semicond.* 39 (3) (2018) 033001.

- [7] P. Iyyappa Rajan, J. Judith Vijaya, S.K. Jesudoss, K. Kaviyarasu, L. John Kennedy, R. Jothiramalingam, H.A. Al-Lohedan, M.Ali Vaali-Mohammed, Green-fuel-mediated synthesis of self-assembled NiO nano-sticks for dual applications-photocatalytic activity on Rose Bengal dye and antimicrobial action on bacterial strains, *Mater. Res. Express* 4 (8) (2017) 085030.
- [8] Prochowicz D, Kornowicz A, Lewiński J (2017) Interactions of Native Cyclodextrins with Metal Ions and Inorganic Nanoparticles: Fertile Landscape for Chemistry and Materials Science, *Chem Rev* 117:13461–13501.
- [9] A. Kalawate, S.C. Sahoo, P.K. Khatua. Compatibility of nanobiocide as wood preservative with thermosetting resin used as adhesive for plywood manufacturing. *International Journal of Composite Materials and Matrices*, 2015, 1(1): 1–6.
- [10] Cloutier, M., Mantovani, D., Rosei, F., “Antibacterial coatings: challenges, perspectives, and opportunities”, *Trends Biotechnol*, 33:637-52 (2015).
- [11] Chidhambaram, N., Ravichandran, K., “Fabrication of ZnO/g-C₃N₄ nanocomposites for enhanced visible light driven photocatalytic activity”, *Mater. Res. Express* 4, 075037 (2017).
- [12] Kolodziejczak, A., Radzimska, and Jesionwska, T., “Zinc oxide from synthesis to application: A review”, *Materials*, 7(4), 2883-2881(2014).
- [13] Ruszkiewicz, J. A., Pinkas, A., Ferrer, B., Peres T. V., Tsatsakis, A., and Aschner, M., “Neurotoxic effect of active ingredients in sunscreen products, a contemporary review”, *Toxicol Rep.* 4:245-259 (2017).
- [14] Samira, B., Chandrappa, K.G., Sharifah, B. A. H., “Facile synthesis of nano-sized ZnO by direct precipitation method”, *Scholars Research Library*, 05, 265-270(2013).
- [15] Surabhi, S. K., Putcha, V., Voonka, Danga R. R., and Gollapalli N. R., “Synthesis, characterization and optical properties of Zinc oxide nanoparticles”, *International Nano letters*, 03, 1-6 (2013).
- [16] Hasnidawani, J. N., Azlina, H.N., Norita, H., Bonnia, N. N., Ratim, S., Ali, F. S., “Synthesis of ZnO nanostructures using sol-gel method synthesis of ZnO nanostructures sol-gel method”, *Procedia Chem.* 19, 211-216 (2016).
- [17] Li, J., Wu, Z., Bao, Y., Chen, Y., Huang, C., Li, N., He, S., and Chen, Z., “Wet chemical synthesis of ZnO nanocoating on the surface of bamboo timber with improved mouldresistance”, *J. Saudi Chem. Soc.* 21, 920-928 (2017).
- [18] Kumar, S.S., Venkateswarlu, P., Rao, V.R., Rao, G.N., “Synthesis, characterization and optical properties of zinc oxide nanoparticles”, *Int. Nano Lett.* 4, 2-6 (2014).
- [19] Abd-Rabboh, H.S.M., Eissa, M., Mohamed, S.K., Hamdy, M.S., “Synthesis of ZnO by thermal decomposition of different precursors: photocatalytic performance under UV and visible light illumination”, *Mater. Res. Express* (2019).
- [20] Navale, S.T., Jadhav, V.V., Tehare, K.K., Sagar, R.U.R., Biswas, C.S., Galluzzi, M., Liang, W., Patil, V.B., Mane, R.S. Stadler, F.J., “Solidstate synthesis strategy of ZnO nanoparticles for the rapid detection of hazardous Cl₂”, *Sens. Actuat. B Chem.* 238, 1102-1110 (2017).
- [21] Bharti, D.B., Bharati, A.V., “Synthesis of ZnO nanoparticles using a hydrothermal method and a study its optical activity”, *Luminescence* 32, 317-320 (2017).
- [22] Rai, P., Kwak, W.K., Yu, Y.T., “Solvothermal synthesis of ZnO nanostructures and their morphology-dependent gas-sensing properties”, *ACS Appl. Mater. Interfaces* 5, 3026-

3032 (2013).

- [23] S. Iravani, Green synthesis of metal nanoparticles using plants, *Green Chem.* 13 (2011) 2638–2650, <https://doi.org/10.1039/C1GC15386B>.
- [24] Nilavukkarasi, M.; Vijayakumar, S.; Prathipkumar, S. Capparis zeylanica mediated biosynthesis of ZnO nanoparticles as antimicrobial photocatalytic and anti-cancer applications. *Mater. Sci. Technol.* 2020, 3, 335–343. [CrossRef]
- [25] Seyyed, M.; Tabrizi, H.M.; Behrouz, E.; Vahid, J. Biosynthesis of pure zinc oxide nanoparticles using Quince seed mucilage for photocatalytic dye degradation. *J. Alloys Compd.* 2020, 821, 153519–153527.
- [26] N.L. Rosi, C.A. Mirkin, Nanostructures in biodiagnostics, *Chem. Rev.* 105 (2005) 1547–1562.
- [27] Xi F-M, Ma S-G, Liu Y-B, Li L and Yu S-S 2016 Artaboterpenoids A and B, bisabolene-derived sesquiterpenoids from *Artabotrys hexapetalus* Org. Lett. 183374–7
- [28] Wong H, Fi and Brown G. D., 2002 β -Methoxy- γ -methylene- α,β -unsaturated- γ -butyrolactones from *Artabotrys hexapetalus* *Phytochemistry* 5999–104
- [29] Iqbal, J. et al. synthesis of green and cost effective cobalt oxide nanoparticles using *Geranium wallichianum* leaves extract and evaluation of in vitro antioxidant, antimicrobial, cytotoxic and enzyme inhibition properties. *Mater. Res. Express.* 6, 115407 (2019).
- [30] Ankamwar, B. Biosynthesis of Gold Nanoparticles (GreenGold) Using Leaf Extract of *Terminalia catappa*. *E-J Chem.* 2010, 7, 1334–1339.
- [31] A.C. Dhanemozhi, V. Rajeswari, S. Sathyajothi, Green synthesis of zinc oxide nanoparticle using green tea leaf extract for supercapacitor application, *Mater. Today Proc.* 4 (2017) 660–667, <http://10.0.3.248/j.matpr.2017.01.070>.
- [32] H. Meruvu, M. Vangalapati, S.C. Chippada, S.R. Bammidi, Synthesis and characterization of zinc oxide nanoparticles and its antimicrobial activity against *Bacillus subtilis* and *Escherichia coli*, *J. Rasayan Chem.* 4 (2011) 217–222.
- [33] Ashwini J., Aswathy T.R., Achuthsankar S. N., Green synthesis and characterization of zinc oxide nanoparticles using *Cayratia pedata* leaf extract, *Biochemistry and Biophysics Reports* 26 (2021) 100995.
- [34] Sekar V., Baskaralingam V., Balasubramanian M., Malaikkarasu S., *Laurus nobilis* leaf extract mediated green synthesis of ZnO nanoparticles: Characterization and biomedical applications, *Biomedicine & Pharmacotherapy* 4 (2016) 1213–1222.
- [35] Soto-Roblesa C.A., Luquea P.A., Gómez-Gutiérrez C.M., Navaa O., Vilchis-Nestor A.R., Lugo-Medina E., Ranjithkumar R., Castro-Beltrán A., Study on the effect of the concentration of *Hibiscus sabdariffa* extract on the green synthesis of ZnO nanoparticles, *Results in Physics* 15 (2019) 102807.
- [36] Kamarajan G., Benny A. D., Porkalai V., Muthuvel A., Nedunchezian G., Mahendran N., Green synthesis of ZnO nanoparticles and their photocatalyst degradation and antibacterial activity, *J. Water Environ. Nanotechnol.*, 7(2): 180–193 Spring 2022.
- [37] Govindasamy S., Marimuthu T., Chandrasekaran M., Green synthesis of ZnO nanoparticles using *Tecoma castanifolia* leaf extract: Characterization and evaluation of its antioxidant, bactericidal and anticancer activities, *Microc* (2018), <https://doi.org/10.1016/j.microc.2018.11.022>.
- [38] Alagesan V., Rangasamy P., Venugopal S., Phytoextract-mediated synthesis of zinc ox-

ide nanoparticles using aqueous leaves extract of *Ipomoea pes-caprae* (L.) R.Br revealing its biological properties and photocatalytic activity, *Nanotechnol. Environ. Eng.* (2017) 2:8 <https://doi.org/10.1007/s41204-017-0018-7>.

[39] Shahla H., Zahra A., Shahram P., Nazi N., Green synthesis of ZnO nanoparticles by Olive (*Olea europaea*), *IET Nanobiotechnol.*, 2016, Vol. 10, Iss. 6, pp. 400–404.

[40] De Souza MM, Madeira A, Berti C, Krogh R, Yunes RA, et al. (2000) Antinociceptive properties of the methanolic extract obtained from *ipomoea pes-Caprae*(L.). *R. Br. J Ethnopharmacol* 69: 85-90.

[41] Devall MS (1992) The biological flora of coastal dunes and wetlands. *Ipomoea pes-caprae* (L.) Roth. *J Coastal Res* 8:442–456.

[42] Nagababu P. and Umamaheswara Rao V. 2015. Pharmacological potential of *Ipomea pes-caprae* (L.) R. Br. Whole plant extracts. *Pelagia Res. Lib.* 6(2): 52-60.

[43] Bragadeeswaran S., Prabhu K., Rani S.S., Priyadharsini S., Vembu N. Biomedical application of beach morning glory *Ipomoea pes-caprae*. *International Journal of Tropical Medicine*, 5; 81–5, (2010).

[44] Nightingale S., Vinoliya J., Mary M., Jilian V. P., Phytochemical Analysis and Biomedical Applications of *Ipomoea pes-caprae* Flower Extract-An In Vitro Study, *International Journal of Pharmacy and Biological Sciences-IJPBSTM* (2019) 9 (1): 275-282.

[45] U. L. Ifeanyichukwu, O. E. Fayemi, and C. N. Ateba, “Green synthesis of zinc oxide nanoparticles from pomegranate (*Punica granatum*) extracts and characterization of their antibacterial activity,” *Molecules*, vol.25,no.19,p.4521,2020.

[46] S. Azizi, R. Mohamad, A. Bahadoran et al., “Effect of annealing temperature on antimicrobial and structural properties of bio-synthesized zinc oxide nanoparticles using flower extract of *Anchusa italica*,” *Journal of Photochemistry and Photobiology B: Biology*, vol. 161, pp. 441–449, 2016.

[47] Adnan A., Abdel-Basit A., Annas A., Al-Hammadi A. H., Waseem S., Pomegranate-Peel Extract-Mediated Green Synthesis of ZnO-NPs: Extract Concentration-Dependent Structure, Optical, and Antibacterial Activity, *Hindawi Journal of Chemistry* Volume 2022, Article ID 9647793, 11 pages <https://doi.org/10.1155/2022/9647793>.

[48] P. Kubelka, F. Munk, “Ein Beitrag zur Optik der Farbanstriche”, *Z. Tech. Phys.*, 12 (1931), 593–601.

[49] P. Kubelka, “New contributions to the optics of intensely light-scattering materials. Part I”, *J. Opt. Soc. Am.*, 38 (1948) 448–457.

[50] M.P. Fuller, P.R. Griffiths, “Diffuse reflectance measurements by infrared Fourier transform spectrometry”, *Anal. Chem.*, 50 (1978) 1906–1910.

[51] Luque PA, Soto-Robles CA, Nava O, Gomez-Gutierrez CM, Castro-Beltran A, Garrafa-Galvez HE, et al. Green synthesis of zinc oxide nanoparticles using *Citrus sinensis* extract. *J Mater Sci Mater Electron* 2018;29:9764–70.

[52] Baneto, M.; Enesca, A.; Lare, Y.; Jondo, K.; Napo, K.; Duta, A. Effect of Precursor Concentration on Structural, Morphological and Opto-Electric Properties of ZnO Thin Films Prepared by Spray Pyrolysis. *Ceram. Int.* 2014, 40, 8397–8404, DOI: 10.1016/j.ceramint.2014.01.048.

[53] Gnanasangeetha D., Sarala T. D., (2013) One pot synthesis of zinc oxide nanoparticles via chemical and green method. *Res J Mater Sci* 1(7):1–8.

- [54] Agarwal H, Kumar SV, Rajeshkumar S (2017) A review on green synthesis of zinc oxide nanoparticles—an eco-friendly approach. *Resour-Eff Technol.* <https://doi.org/10.1016/j.reffit.2017.03.002>
- [55] Lallo da Silva, B., Caetano, B., Chiari-Andreo, B. G., Pietro, R. C. L., Chiavacci, L. A., “Increased antibacterial activity of ZnO nanoparticles: influence of size and surfacemodification”, *Colloids Surf B Biointerfaces* (2019) 177:440-7.
- [56] Yusof, N.A.A., Zain, N.M., Pauzi, N., “Synthesis of ZnO nanoparticles with chitosan as stabilizing agent and their antibacterial properties against Gram-positive and Gram-negative bacteria”, *Int J Biol Macromol* (2019) 124:1132–6.
- [57] Zhong, L., Liu, H., Samal, M., Yun, K., “Synthesis of ZnO nanoparticles-decorated spin-dleshaped graphene oxide for application in synergistic antibacterial activity”, *J Photochem Photobiol B* (2018) 183:293–301.
- [58] Kashef, N., Huang, Y.Y., Hamblin, M.R., “Advances in antimicrobial photodynamic in-activation at the nanoscale,” *Nanophotonics* (2017) 6(5):853–79.
- [59] Bhakta D., Ganjewala D. Effect of leaf positions on total phenolics, flavonoids and proanthocyanidins content and antioxidant activities in *Lantana camara* (L). *Journal of Scientific Research*, 1(2); 363-369, (2009).
- [60] Bharathi D, Bhuvaneshwari V (2019) Synthesis of zinc oxide nanoparticles (ZnO-NPs) using pure bioavonoid rutin and their biomedical applications: antibacterial, antioxidant and cytotoxic activities. *Res. Chem. Intermed* 45: 2065–2078. <https://doi.org/10.1007/s11164-018-03717-9>
- [61] Sunanda K, Kikuchi Y, Hashimoto K, Fujishima A (1998) Bactericidal and detoxification effects of TiO₂ thin film photocatalysts. *Environ Sci Technol* 32(1998):726–728.
- [62] Jamdagni, P. Khatri, J.S. Rana, Green synthesis of zinc oxide nanoparticles using flower extract of *Nyctanthes arbor-tristis* and their antifungal activity, *J. King Saud Univ. Sci.* 30 (2018) 168–175, <http://10.0.3.248/j.jksus.2016.10.002>.
- [63] O.T. Jemilugba, El.Hadji Mamour Sakho, S. Parani, V. Mavumengwana, O.S. Oluwafemi, Green synthesis of silver nanoparticles using *Combretum erythrophyllum* leaves and its antibacterial activities, *Colloid Interface Sci. Commun.* 31 (2019) 100191.
- [64] El.Hadji Mamour Sakho, J. Jose, S. Thomas, N. Kalarikkal, O.S. Oluwafemi, Antimicrobial properties of MFe₂O₄ (M=Mn, Mg)/reduced graphene oxide composites synthesized via solvothermal method, *Mater. Sci. Eng.* 95 (2019) 43–48.
- [65] O.S. Oluwafemi, T. Mochochoko, A. John Leo, S. Mohan, S.P. Songca, Microwave irradiation synthesis of silver nanoparticles using cellulose from *Eichhornia crassipes* plant shoot, *Mater. Lett.* 185 (2016) 576–579.